

# Observations of the Centaur 1999 UG<sub>5</sub>: Evidence of a Unique Outer Solar System Surface

JAMES M. BAUER,<sup>1</sup> KAREN J. MEECH, AND YANGA R. FERNÁNDEZ

Institute for Astronomy, University of Hawaii, 2680 Woodlawn Drive, Honolulu, HI 96822

TONY L. FARNHAM

University of Texas, Department of Astronomy, Austin, TX 78712

AND

TED L. ROUSH

Space Science Division, Planetary Systems Branch, Mail Stop 245-3, NASA Ames Research Center, Moffet Field, CA 94035-1000

*Received 2002 July 19; accepted 2002 August 30; published 2002 November 12*

**ABSTRACT.** The outer solar system body 1999 UG<sub>5</sub> is a Centaur of medium brightness and slightly redder color when compared to other Centaurs. Similar to at least  $\frac{1}{5}$  of the known Centaurs, it is a Saturn-crosser with a mean orbital distance between Saturn and Uranus. We present optical photometry data and near-IR spectra obtained during 2000 September, November, and December. We find a rotation period of  $13.41 \pm 0.04$  hr with an amplitude of  $0.102 \pm 0.005$  mag and a phase curve with a Lumme-Bowell  $G$  value of  $-0.13 \pm 0.02$ .  $BVR$ I colors are reported, and they confirm the red spectral gradient observed previously. Our spectra reveal that this redward slope extends into near-IR wavelengths and indicates possible localized differences in the surface composition.

## 1. INTRODUCTION

Centaurs inhabit an inherently unstable region of our solar system (Holman & Wisdom 1993) located between 5 and 30 AU. They are often speculated to be objects in transition from the Kuiper belt, as their orbits dynamically evolve into short-period comet orbits or they get ejected from the solar system. As such, they are believed to contain many volatiles, in ice form, with surfaces possibly darkened by long exposures to cosmic-ray radiation over the life of the solar system (e.g., Strazzulla & Johnson 1991). As of 2002 August, there are about 37 known members of this class out of a projected population of  $2 \times 10^3$  (for bodies with radius  $r_N > 25$  km; Jedicke & Herron 1997; Sheppard et al. 2000). To date a handful of the brightest of these objects have been studied using near-infrared (NIR) spectroscopy (see Table 1), and many have been shown to exhibit water-ice features. With one disputed observation (Kern et al. 2000; Romon-Martin et al. 2001), surface variations detected at NIR wavelengths are rare, and correlations to observations of variations at optical wavelengths are even rarer. In order to characterize potential surface variations on the Centaurs, we have performed simultaneous NIR and optical observations on several targets; 1999 UG<sub>5</sub> was one of our earlier targets for NIR spectroscopy. 1999 UG<sub>5</sub> is by appearances a rather common Centaur object. Its  $H_V$  value is reported as

$10.42 \pm 0.02$  (Gutiérrez et al. 2001) and, with an assumed 5% albedo, the diameter is 55 km. It has an elliptical orbit ( $e = 0.42$ ) and has a mean orbital distance outside Saturn's orbit ( $a = 12.8$  AU). Peixinho et al. (2001) and Gutiérrez et al. (2001) have reported a light-curve variation with a total range of  $\sim 0.24 \pm 0.02$  mag and a period of 13.25 hr and imply a resulting minimum axial ratio of 1.25. With a reported  $V-R$  color of 0.63, 1999 UG<sub>5</sub> is among the redder of the Centaur objects but is not the reddest, as C/2001 T<sub>4</sub> has a  $V-R$  color of  $\sim 0.9$  (Bauer et al. 2001), and Pholus has a color of  $V-R = 0.8$  (Buie & Bus 1992). Our own UH Centaur color survey (Bauer et al. 2001) does not indicate that 1999 UG<sub>5</sub> has a particularly unique color. Neither is it particularly unique that the Centaur has a detectably large light-curve amplitude, as at least six others, out of a total of about 37 observed, have shown light curves with regular periodicity.

It is important to sort out which combinations of NIR and optical observable characteristics are true indicators of young and old surfaces. Organic molecules, when exposed to charged particles and UV radiation, produce radiolysis and photolysis by-products. Laboratory evidence shows that carbon-containing frozen mixtures will form complex organics when exposed to radiation, which will break down under irradiation by cosmic rays (Strazzulla & Johnson 1991). The effects of progressive irradiation include weakening of the CH bond IR absorption bands, a change in the slope of the visible reflectance spectrum ( $0.4\text{--}0.8 \mu\text{m}$ ), and a lowering of the albedo. Hence, there is much speculation that red outer solar system materials result

---

<sup>1</sup> Visiting Astronomer, NASA Infrared Telescope Facility (IRTF), Institute for Astronomy, Honolulu, HI.

TABLE 1  
OPTICAL LIGHT CURVES AND NIR SPECTRA OF CENTAURS

Object	Light-Curve Reference <sup>a</sup>	Period and Amplitude <sup>b</sup>	NIR Spectrum Reference <sup>c</sup>
Chiron .....	1	5.9, 0.3	1
Pholus .....	2	9.98, 0.1	2
Chariklo .....	...	...	3
Asbolus .....	3	8.9, 0.3	4
1998 BU <sub>48</sub> .....	4	4–6, 0.68	...
1999 UG <sub>5</sub> .....	5	13.41, 0.102	...
2001 PT <sub>13</sub> .....	6	8.338, 0.15	5
2000 QC <sub>243</sub> .....	7	9.14, 0.4	...

<sup>a</sup> First reference of light-curve observations.

<sup>b</sup> Current known rotation period (hours) and amplitude ( $\Delta$ mag).

<sup>c</sup> First reference of NIR spectrum.

REFERENCES.—Light curves: (1) Bus, Bowell, & French 1988; (2) Buie & Bus 1992; (3) Brown & Luu 1997; (4) S. S. Sheppard & D. C. Jewitt 2002, in preparation; (5) Gutiérrez et al. 2001; (6) Farnham 2001 (see also Farnham & Davies 2002); (7) Ortiz et al. 2002. NIR spectra: (1) Foster et al. 1999; (2) Cruikshank et al. 1998; (3) Brown & Koresko 1998; (4) Barrucci, Lazzarin, & Tozzi 1999; (5) Barrucci et al. 2002.

from these processes (Strazulla & Johnson 1991; Tegler & Romanishin 2000) and that bright, neutral-blue surfaces correspond to newly exposed icy surfaces (Stern 1995; Hainaut et al. 2000). Yet radiation processing may affect these surfaces differently depending on the original composition.

## 2. OBSERVATIONS

### 2.1. Photometry

We obtained data at the University of Hawaii (UH) 2.2 m telescope on 2000 August 2, September 22, November 8, and December 18–22 (UT). The images were obtained using the Tek 2048 CCD camera. We also obtained a second set of data

TABLE 2  
OPTICAL OBSERVING CONDITIONS

Date	$r$ (AU)	$\Delta$ (AU)	$\alpha$ (deg)	Seeing (arcsec FWHM)	Conditions
2000 Aug 2 .....	8.082	7.850	7.1	1.5	Photometric
2000 Sep 21 .....	7.910	7.364	6.3	1	Cirrus
2000 Sep 22 .....	7.911	7.353	6.3	1	Cirrus
2000 Nov 1 .....	7.964	7.015	2.2	~4	Cirrus
2000 Nov 2 .....	7.965	7.011	2.1	<3	Photometric
2000 Nov 8 .....	7.974	6.998	1.3	1	Photometric
2000 Dec 18 .....	8.029	7.190	3.9	1.1	Photometric
2000 Dec 19 .....	8.031	7.200	4.0	0.9	Photometric
2000 Dec 20 .....	8.033	7.212	4.1	1.1	Photometric
2000 Dec 21 .....	8.034	7.225	4.2	1.1	Photometric

on 2000 November 1–2 at the McDonald Observatory 0.76 m telescope and an additional set of data at the UH 2.2 m telescope on 2001 October 29. The geometry and observing conditions are included in Table 2, and those of the instrumentation are in Table 3. The data were bias subtracted and flattened in the usual manner, and standard-star measurements (Landolt 1992) were used to obtain zero-point offsets, atmospheric absorption coefficients, and color-correction terms for the filter sets for each photometric night. Table 4 contains the *BVR*-band photometry values of 1999 UG<sub>5</sub> observations and UT times. Typical exposure times for all our data sets were on the order of 600 s. The uncertainties listed in the table are the combined uncertainties from the photon-counting statistics for each exposure and the uncertainties in the derived extinction coefficients and zero-point offsets from each night. For the nights such as November 1, where differential photometry was used to derive the Centaur magnitude values, the average uncertainties in the reference star photometry values, although comparatively small, were also folded in. Light travel time and geo-

TABLE 3  
OBSERVING INSTRUMENTS

Date	Telescope <sup>a</sup>	Detector	Slit Size/Aperture <sup>b</sup> (arcsec)	Plate Scale (arcsec pixel <sup>-1</sup> )	Read Noise (e <sup>-</sup> pixel <sup>-1</sup> )	Gain (e <sup>-</sup> ADU <sup>-1</sup> )
2000 Aug 2 .....	UH 2.2 m	8K Mosaic	10	0.26	8	2
2000 Sep 21 .....	IRTF	SpeX	0.8	0.15	<1	14
2000 Sep 22 .....	IRTF	SpeX	0.8	0.15	<1	14
	UH 2.2 m	Tek 2048	7 <sup>c</sup>	0.22	6	1.74
2000 Nov 1 .....	MO 0.76 m	Loral 2048	8 <sup>c</sup>	1.34	6	1.6
2000 Nov 2 .....	MO 0.76 m	Loral 2048	8 <sup>c</sup>	1.34	6	1.6
2000 Nov 8 .....	UH 2.2 m	Tek 2048	7 <sup>c</sup>	0.22	6	1.74
2000 Dec 18 .....	UH 2.2 m	Tek 2048	7 <sup>c</sup>	0.22	6	1.74
2000 Dec 19 .....	UH 2.2 m	Tek 2048	5 <sup>c</sup>	0.22	6	1.74
2000 Dec 20 .....	UH 2.2 m	Tek 2048	5 <sup>c</sup>	0.22	6	1.74
2000 Dec 21 .....	UH 2.2 m	Tek 2048	5 <sup>c</sup>	0.22	6	1.74
2001 Oct 29 .....	UH 2.2 m	Tek 2048	5 <sup>c</sup>	0.22	6	1.74

<sup>a</sup> UH 2.2 m = University of Hawaii 2.2 m telescope on Mauna Kea; IRTF = NASA 3 m Infrared Telescope Facility on Mauna Kea; MO = McDonald Observatory 0.76 m.

<sup>b</sup> Slit size for SpeX or photometry aperture used for CCD analysis.

<sup>c</sup> Magnitudes were corrected for signal loss due to seeing and aperture size variation using differential photometry.

TABLE 4  
PHOTOMETRY

UT	Filter	Magnitude	$\pm\sigma$	UT	Filter	Magnitude	$\pm\sigma$	UT	Filter	Magnitude	$\pm\sigma$
2000 Aug 02 = 2,541,760.5 HJD				2000 Nov 02 = 2,451,850.5 HJD				2000 Dec 19 = 2,451,899.5 HJD			
14.4892	R	19.431	0.052	7.3366	R	18.786	0.029	6.3122	V	19.578	0.007
14.5975	V	20.080	0.074	7.5289	I	18.248	0.036	6.5631	R	18.906	0.017
14.7108	R	19.451	0.052	7.9369	B	20.474	0.115	6.7964	I	18.320	0.009
2000 Sep 22 = 2,541,809.5				2000 Nov 08 = 2,451,856.5				2000 Dec 20 = 2,451,900.5			
9.3194	V	19.962	0.037	8.1289	R	18.775	0.030	7.0356	R	18.898	0.017
9.3911	V	20.009	0.038	9.6169	R	18.690	0.032	7.265	R	18.908	0.017
9.6044	I	18.737	0.034	9.8329	I	18.162	0.044	7.4914	R	18.894	0.017
9.6742	I	18.706	0.032	10.0249	V	19.418	0.054	7.7014	R	18.881	0.017
9.8206	R	19.208	0.021	10.2169	B	20.129	0.076	7.9347	R	18.888	0.017
9.8925	R	19.273	0.022	10.4089	R	18.640	0.029	8.1644	R	18.884	0.009
9.9622	R	19.155	0.020	11.3689	R	18.660	0.035	8.3944	R	18.888	0.009
10.0319	R	19.245	0.021	11.5849	V	19.383	0.050	8.6144	R	18.885	0.014
10.1050	R	19.227	0.021	11.7771	R	18.608	0.027	8.8456	R	18.915	0.014
12.4167	R	19.145	0.019	10.3725	R	18.662	0.025	9.0606	R	18.889	0.014
12.5236	R	19.123	0.019	10.4425	R	18.658	0.027	9.2747	R	18.877	0.009
12.6872	R	19.158	0.019	10.5122	R	18.659	0.039	9.4875	R	18.876	0.014
12.7586	R	19.158	0.019	10.5822	V	19.314	0.050	9.7106	R	18.887	0.017
12.8283	R	19.123	0.018	10.6589	V	19.298	0.048	10.7022	R	18.900	0.018
12.8983	R	19.092	0.018	10.7289	V	19.344	0.052	10.9403	R	18.911	0.023
12.9681	R	19.131	0.018	2000 Dec 18 = 2,451,898.5				11.1514	R	18.887	0.009
13.0378	R	19.113	0.018	6.5011	R	18.915	0.016	11.3658	R	18.880	0.009
13.8736	I	18.572	0.028	6.5831	I	18.315	0.013	2000 Dec 21 = 2,451,901.5			
13.9447	I	18.548	0.027	6.6625	V	19.582	0.013	9.6928	R	18.912	0.009
13.5917	V	19.800	0.026	6.7758	R	18.795	0.015	9.9233	R	18.902	0.009
13.6614	V	19.937	0.028	6.8792	I	18.297	0.012	10.1761	R	18.888	0.009
13.7339	R	19.082	0.017	6.9606	V	19.573	0.013	10.3892	R	18.894	0.009
13.8039	R	19.109	0.018	7.1278	R	18.859	0.010	10.605	R	18.910	0.018
14.0147	R	19.074	0.018	7.3897	R	18.861	0.010	10.9503	R	18.919	0.029
14.0844	R	19.091	0.018	7.5975	R	18.913	0.010	11.1639	R	18.908	0.018
14.1542	R	19.053	0.017	7.8231	R	18.907	0.010	2000 Dec 21 = 2,451,901.5			
14.2242	R	19.070	0.017	8.0517	R	18.874	0.010	5.7467	R	19.058	0.010
14.2939	R	19.065	0.017	8.2639	R	18.898	0.009	5.9719	R	19.065	0.010
14.3639	R	19.041	0.017	8.4800	R	18.890	0.009	7.3097	R	19.022	0.014
14.4336	R	19.074	0.017	8.6850	R	18.904	0.009	7.5181	R	19.060	0.014
14.5033	R	19.045	0.017	8.9000	R	18.902	0.009	7.7511	R	19.080	0.015
14.5733	R	19.067	0.017	9.1169	R	18.898	0.009	7.9631	R	19.043	0.017
14.7131	R	19.078	0.017	9.3231	R	18.918	0.009	8.1875	R	19.078	0.019
14.7828	R	19.097	0.018	10.0928	R	18.957	0.010	8.3944	R	19.090	0.017
14.8525	R	19.022	0.017	10.6406	R	18.968	0.011	8.8622	R	19.039	0.019
14.9225	R	19.065	0.017	10.8592	R	18.974	0.011	9.0678	R	19.061	0.014
14.9922	R	19.048	0.017	11.0700	R	19.004	0.012	9.2914	R	19.046	0.014
15.0622	R	19.066	0.018	11.2881	R	19.000	0.013	9.5256	R	19.024	0.012
2000 Nov 01 = 2,451,849.5				2000 Dec 18 = 2,451,898.5				2000 Dec 21 = 2,451,901.5			
7.8914	R	18.656	0.029	11.5106	R	18.988	0.013	9.7306	R	18.979	0.012
8.2994	R	18.672	0.034	2000 Dec 21 = 2,451,901.5				9.9561	R	18.994	0.012
10.0994	R	18.627	0.039	2000 Dec 21 = 2,451,901.5				10.1742	R	18.987	0.012
10.2914	V	19.395	0.065	2000 Dec 21 = 2,451,901.5				10.3819	R	18.971	0.012
10.5077	R	18.637	0.038	2000 Dec 21 = 2,451,901.5				2001 Oct 29 = 2,452,211.5			
11.8757	R	18.718	0.050	2000 Dec 21 = 2,451,901.5				14.9400	R	19.269	0.017
2000 Nov 01 = 2,451,849.5				2000 Dec 21 = 2,451,901.5				15.0197	I	18.653	0.025
2000 Nov 01 = 2,451,849.5				2000 Dec 21 = 2,451,901.5				15.1042	R	19.237	0.017
2000 Nov 01 = 2,451,849.5				2000 Dec 21 = 2,451,901.5				15.2100	V	19.903	00.027

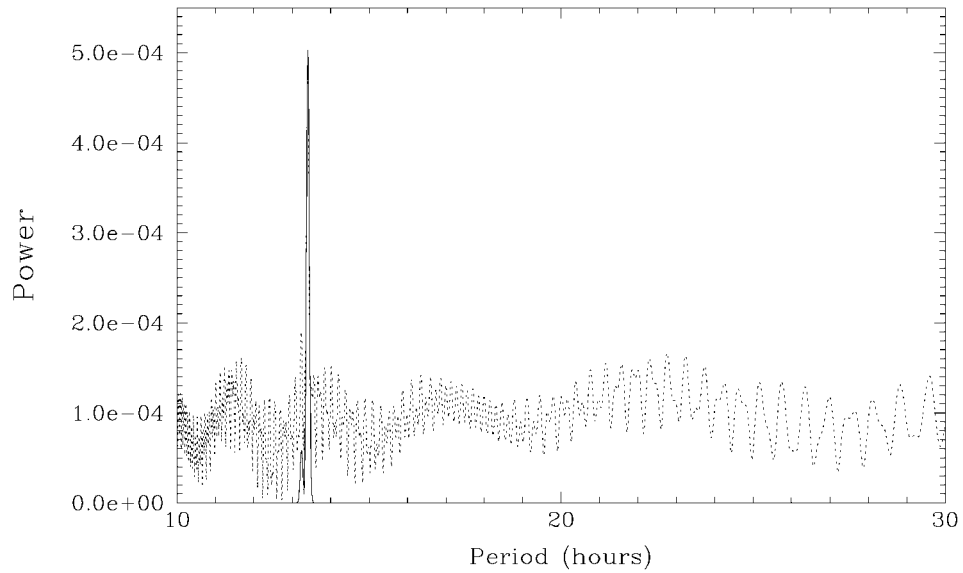


FIG. 1.—Fourier spectra for the rotation search, cleaned of the sampling residuals (*solid line*), and raw (*dashed line*, rescaled to one-third its original value). Note the unambiguous maximum peak at 13.41 hr in both spectra.

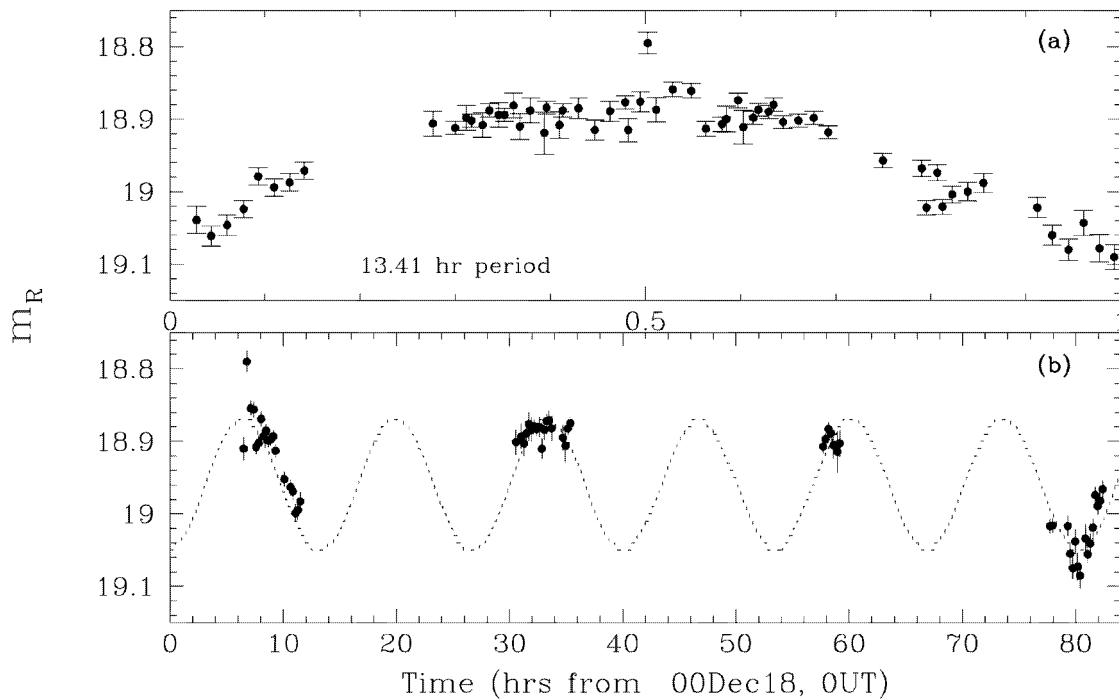


FIG. 2.—(a) 2000 December data phased to a period value of 13.41 hr. (b) Data graphed over the 4 day observation span (in hours), with a sine curve of 0.1 mag amplitude and 13.41 hr period superposed.

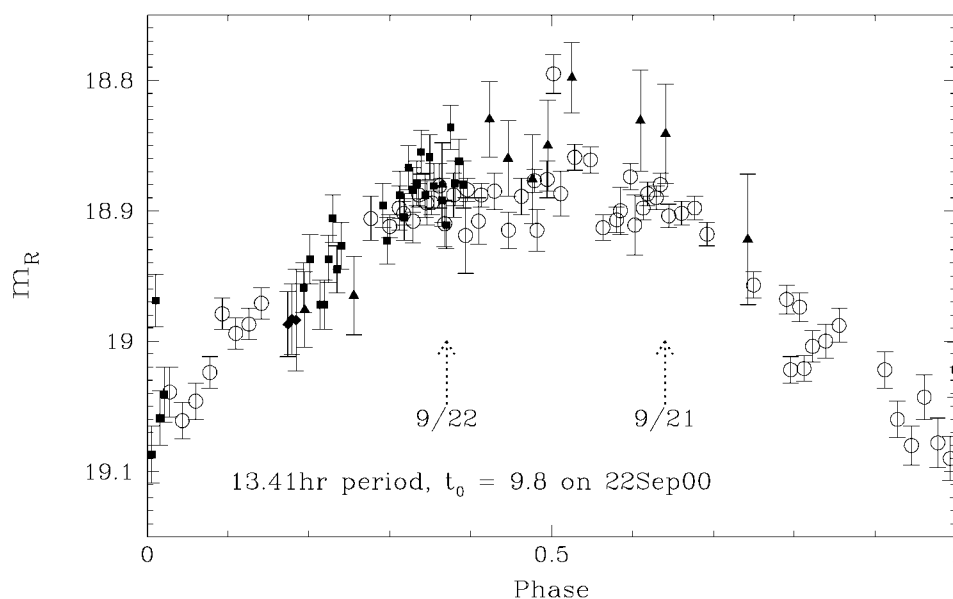


FIG. 3.—Data from 2000 December 18–21 (*open circles*), November 1–2 (*filled triangles*), November 8 (*filled diamonds*), and September 22 (*filled squares*), phased to a 13.41 hr period. The minimum occurred at approximately 9.8 UT, 2000 September 22 (uncorrected for light travel time). Arrows indicate the phases of our spectral data from September 21 (rotational phase of 0.37) and September 22 (0.64).

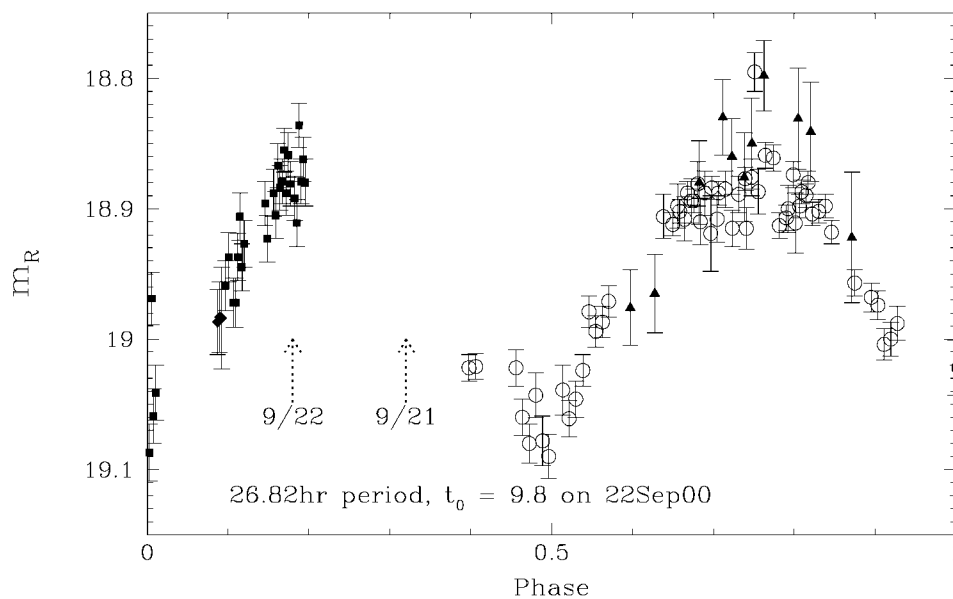


FIG. 4.—Data from 2000 December 18–21 (*open circles*), November 1–2 (*filled triangles*), November 8 (*filled diamonds*), and September 22 (*filled squares*), phased to a 26.82 hr period. The minimum occurred at approximately 9.8 UT, 2000 September 22 (uncorrected for light travel time). Arrows indicate the mean phase of our spectral data from September 21 (rotational phase of 0.51) and September 22 (0.37). Note the lack of coverage on the first peak and the persistence of the asymmetric shape of the second.

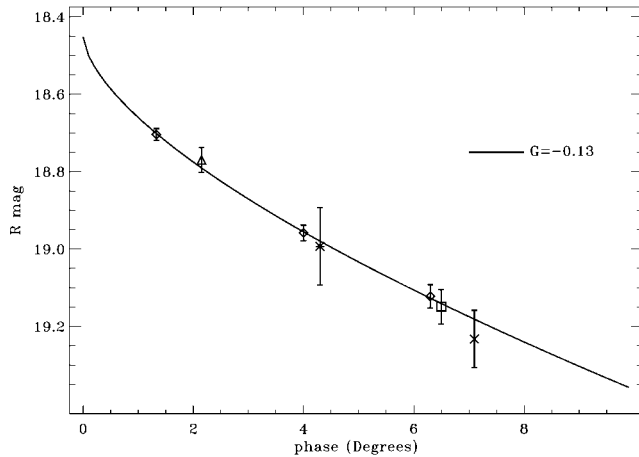


FIG. 5.—Final phase fits to the rotation light-curve corrected magnitudes for our three UH data sets from 2000 September–December (*diamonds*), our McDonald Observatory data set (*triangles*), plus the data minimum reported by Gutiérrez et al. (2001) on 2001 January 21 (*square*). The error bars of the 2001 January 21 point is the combined uncertainty of the original error and that introduced in calibration to our data. Additional points from 2000 August 2 (*cross*) and 2001 October 29 (*asterisk*) were not included in the fit but are shown here for comparison

metric corrections have not been made in the data shown here but were made subsequently for the period search (see § 3).

2000 August 2 was photometric, but observations of 1999 UG<sub>5</sub> were taken close to twilight and hence had a large uncertainty owing to photon noise from the high sky background. Light cirrus was present during our observations on 2000 September 22, so we recalibrated the magnitudes of background stars in our fields during other photometric nights at the telescopes. We measured the magnitudes of four field stars and

TABLE 5  
FILTER SET CONVERSION PARAMETERS

Filter	Bessel $\lambda_{\text{eff}}$ ( $\mu\text{m}$ )	UH $\lambda_{\text{eff}}$ ( $\mu\text{m}$ )	UH Color Offset
R .....	0.6390	0.6454	
V .....	0.5384	0.5412	$\delta_{V-R} \approx +0.022$
I .....	0.8092	0.8143	$\delta_{R-I} < 0.01 (\approx 0.00)$

calculated the magnitude of 1999 UG<sub>5</sub> from the weighted average of the relative offsets from these field standards in each frame from 2000 September 22. For the McDonald Observatory observing run on 2000 November 1–2, the observing conditions on November 1 were poor. It was only partly photometric and the seeing was greater than 4" and variable. November 2 was photometric and had seeing less than 3". Because of the poor quality of the night of November 1, we used relative photometry to produce the initial measurements, with the same reference stars for both nights, and used the comparison stars on November 2 to shift all of the magnitudes to the standard star system. By using this method to correct the November 1 Centaur magnitude values, the signal falling outside the photometry apertures owing to seeing variations would be the same for both the Centaur and the frame standards and would be accounted for in the frame reference standard offsets for each exposure. As 1999 UG<sub>5</sub> was at a relatively low Galactic latitude ( $\sim -30^\circ$ ), and as the McDonald Observatory's camera had a relatively large field of view (1.3 pixel<sup>-1</sup> scale), there were sufficient isolated frame standards available to apply this technique with reasonable accuracy. In order to check the accuracy of the 2000 December photometry from night to night, we sampled three stars that overlapped on the frames from December 18 and 19 and three stars that overlapped on the

TABLE 6  
OPTICAL PHOTOMETRY COLORS (BESSEL) AND GRADIENTS

Date	B–V ( $\pm\sigma$ )	V–R ( $\pm\sigma$ )	R–I ( $\pm\sigma$ )	Rotational Phase
2000 Aug 2, 14.6 UT .....	...	0.64 ( $\pm 0.09$ )	...	0.66
2000 Aug 2 gradient [% (0.1 $\mu\text{m}$ ) <sup>-1</sup> ] .....	...	28 ( $\pm 9$ )	...	
2000 Sep 22, 9.5 UT .....	...	0.720 ( $\pm 0.03$ )	0.52 ( $\pm 0.03$ )	0.98
2000 Sep 22, 13.7 UT .....	...	0.73 ( $\pm 0.02$ )	0.55 ( $\pm 0.02$ )	0.29
2000 Sep 22 average .....	...	0.73 ( $\pm 0.02$ )	0.54 ( $\pm 0.02$ )	
2000 Sep 22 gradient [% (0.1 $\mu\text{m}$ ) <sup>-1</sup> ] .....	...	39 ( $\pm 3$ )	16 ( $\pm 1$ )	
2000 Nov 1, 10.2 UT .....	...	0.76 ( $\pm 0.07$ )	...	0.62
2000 Nov 2, 9.9 UT .....	0.941 ( $\pm 0.131$ )	0.75 ( $\pm 0.06$ )	0.53 ( $\pm 0.04$ )	0.38
2000 Nov 2, 11.5 UT .....	0.715 ( $\pm 0.097$ )	0.75 ( $\pm 0.06$ )	0.50 ( $\pm 0.05$ )	0.50
2000 Nov 1–2, average .....	0.795 ( $\pm 0.081$ )	0.75 ( $\pm 0.04$ )	0.52 ( $\pm 0.03$ )	
2000 Nov 1–2 gradient [% (0.1 $\mu\text{m}$ ) <sup>-1</sup> ] .....	[15 ( $\pm 9$ )]	43 ( $\pm 4$ )	14 ( $\pm 2$ )	
2000 Nov 8, 10.6 UT .....	...	0.68 ( $\pm 0.03$ )	...	0.19
2000 Nov 8 gradient [% (0.1 $\mu\text{m}$ ) <sup>-1</sup> ] .....	...	33 ( $\pm 4$ )	...	
2000 Dec 18, 7 UT .....	...	0.63 ( $\pm 0.02$ )	0.61 ( $\pm 0.01$ )	0.52
2000 Dec 19, 6.8 UT .....	...	0.64 ( $\pm 0.02$ )	0.59 ( $\pm 0.01$ )	0.28
2000 Dec 18–19, average .....	...	0.64 ( $\pm 0.01$ )	0.60 ( $\pm 0.01$ )	
2000 Dec 18–19 gradient [% (0.1 $\mu\text{m}$ ) <sup>-1</sup> ] .....	...	28 ( $\pm 1$ )	20 ( $\pm 1$ )	
2001 Oct 29, 15 UT .....	...	0.67 ( $\pm 0.03$ )	0.60 ( $\pm 0.03$ )	...
2001 Oct 29 gradient [% (0.1 $\mu\text{m}$ ) <sup>-1</sup> ] .....	...	32 ( $\pm 4$ )	20 ( $\pm 4$ )	

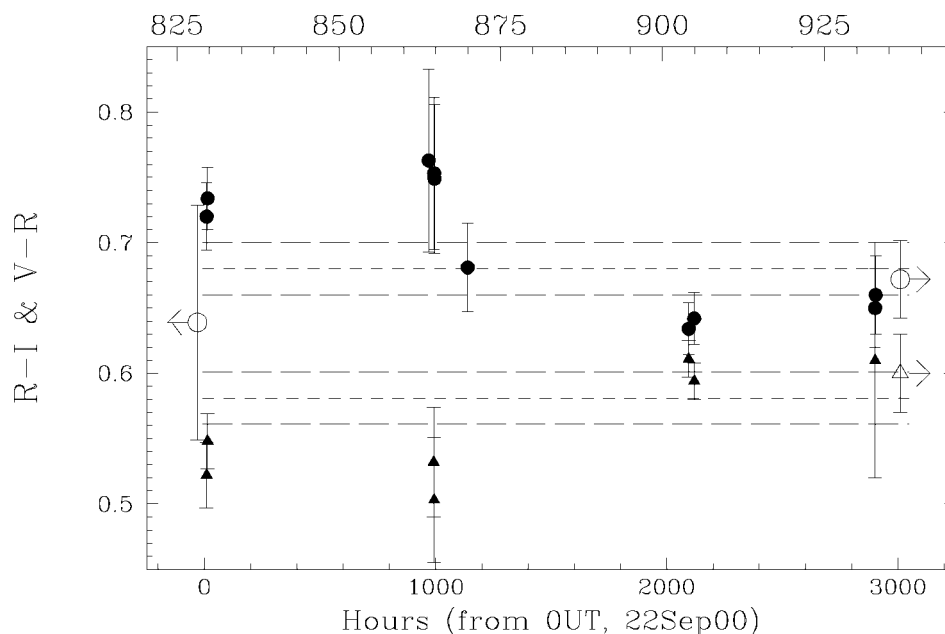


FIG. 6.—1999 UG<sub>5</sub> colors of with  $V-R$  (circles) and  $R-I$  (triangles) graphed vs. time. The open symbols on the left and right of the graph represent the data taken on 2000 August 2 and 2001 October 29, respectively. The dashed lines represent the weighted average (short-dashed) and errors (long-dashed) of all of our  $V-R$  (upper) and  $R-I$  (lower) colors.

frames from December 19, 20, and 21. For the nights of December 19–20, the average photometry values for our three field standards varied within 0.001 mag. In the case of December 21, we found an average magnitude value offset of +0.03, so we compensated for it by subtracting that value from the magnitudes. Similarly, we found an offset of  $-0.007$  mag for the night of December 18 and corrected our Centaur magnitudes. These magnitude adjustments had little or no effect on our period-search analysis below, but they did affect the shape of the phased light curve by lowering the amplitude and eliminating obvious night-to-night discontinuities in the phased data (see § 3). Observations taken on 2001 October 29 were made during photometric conditions and provided color and absolute magnitude information.

## 2.2. Spectroscopy

We obtained spectra on two separate nights, 2000 September 21 and 22, at the NASA Infrared Telescope Facility (IRTF) using the SpeX instrument (J. T. Rayner et al. 2002, in preparation) in PRISM mode. On the 21st, we received only a fraction of the night as a test of the SpeX instrument, since the time was originally allocated as engineering time. Hence, our first night’s spectrum had a total integration time of 600 s and had a midpoint time of 15.60 UT. Our second night’s data were for a total integration time of 4320 s and had a midpoint time of 14.75 UT. The September 22 data were obtained simultaneously with the UH 2.2 m photometry data for that night. On both nights we used a  $0''.8$  slit width, and the nominal seeing was  $\sim 1''$ . This gave us a wavelength resolution of  $\sim 0.016 \mu\text{m}$

while collecting more than half the signal flux from our object. We used observations of the G5 V solar analog standard star HR 1262 (Gaidos 1998), obtained before and after the object measurements, for flux calibration and to correct for atmospheric absorption. The standard was in the same region of the sky and shared the same air mass within a few hundredths of our observations. We nodded the telescope  $7''$  between exposures and used on-frame subtraction to eliminate the sky background.

## 3. ANALYSIS

### 3.1. Photometry

We first employed a phase dispersion minimization (PDM; Stellingwerf 1978) technique to determine possible rotation periods from our 2000 December data set. The PDM technique minimizes the variance of the data that has been converted to a phase for each trial period and grouped into bins. The  $\Theta$ -statistic, as defined by Stellingwerf, is a ratio of the total data variance to the combined bin variance (Stellingwerf 1978; Bevington 1969). The technique indicates periodicity in the data by minima in the  $\Theta$ -values. Minima near 8, 16, and 24 hr, in consideration of our strong sampling bias on the order of these periods, were not likely candidates. The significant minima in the PDM converge to  $\Theta$ -values of less than 1.0, which the minima near 8 and 16 hr did not do. However, we found a strong minimum near 13.1 hr. From the width of PDM minimum, we estimated our uncertainty for this single-peaked light-curve period at near  $\pm 0.3$  hr.

TABLE 7  
MODEL FITS TO 1999 UG<sub>5</sub> DATA

Spectra	Component	Mass Fraction	Grain Size (μm)	Reduced <sup>a</sup> χ <sup>2</sup>
2000 September 21, 15.60 UT				
Model 1 .....	Amorphous H <sub>2</sub> O ice	0.17	66	2.97
	Amorphous carbon	0.41	154	
	Triton tholin	0.42	28	
Model 2 .....	Amorphous H <sub>2</sub> O ice	0.29	78	3.46
	Amorphous carbon	0.26	131	
	Triton tholin	0.39	44	
	NH <sub>3</sub> ice	0.06	92	
Model 3 .....	Amorphous H <sub>2</sub> O ice	0.26	70	3.42
	Amorphous carbon	0.39	71	
	Triton tholin	0.34	24	
	Methanol ice	0.01	32	
Model 4 .....	Amorphous H <sub>2</sub> O ice	0.04	8	6.79
	Amorphous carbon	0.50	114	
	Titan tholin	0.39	41	
	Olivine	0.07	43	
Model 5 .....	Amorphous H <sub>2</sub> O ice	0.03	40	7.36
	Amorphous carbon	0.56	63	
	Methanol ice	0.03	7	
	Titan tholin	0.31	15	
	Olivine	0.07	75	
2000 September 22, 14.75 UT				
Model 1 .....	Amorphous H <sub>2</sub> O ice	0.14	48	5.12
	Amorphous carbon	0.79	67	
	Triton tholin	0.07	11	
Model 2 .....	Amorphous H <sub>2</sub> O ice	0.13	115	3.04
	Amorphous carbon	0.66	27	
	Titan tholin	0.14	10	
	Methanol ice	0.03	15	
	Olivine	0.04	93	
Model 3 .....	Amorphous H <sub>2</sub> O ice	0.06	24	4.26
	Amorphous carbon	0.83	142	
	Titan tholin	0.09	45	
	NH <sub>3</sub> ice	<0.01	59	
	Olivine	0.02	111	

<sup>a</sup> See Bevington 1969 for definition.

In order to properly temporally phase the data from the other observing runs and thus obtain a more precise measure of the period, one needs to know the phase-angle behavior so as to put all data sets on a common magnitude scale. However, the phase-angle behavior, encapsulated by the Lumme-Bowell parameter  $G$  (Bowell et al. 1989), cannot be found without understanding the rotational amplitude and the period. Thus, the rotation state and phase-angle behavior are intimately tied together in terms of the photometry. Shifting the photometry data to a conventional  $H_V(1, 0)$  reference frame would require adding relatively large uncertain offset values. Consequently, throughout the period search and viewing angle analysis, we used our December 18 observation geometry as the reference frame and so avoided introducing larger geometric and phase-angle offsets in the data. By keeping the photometry values in

the  $R$  band, we avoided making uncertain color offsets. We made only small adjustments of less than 0.08 in magnitude for differences in the heliocentric and geocentric distances from 2000 September 22 through December 21 relative to 2000 December 18. We made phase corrections relative to  $4^\circ$  and thus avoided adding larger phase offsets dependent on mostly uncertain values, such as the magnitude of the opposition surge at  $0^\circ$ . This still required a small viewing angle phase-curve adjustment of the September 22 and November 1, 2, and 8 data. As an initial attempt, using the ephemeris values obtained from JPL<sup>2</sup> (the source of our orbital elements as well), and removing the geometric brightening owing to the difference in geocentric ( $\Delta/\Delta_{12/18}$ ) and heliocentric ( $r/r_{12/18}$ ) distances of 1999 UG<sub>5</sub> at the times of observation, we assume a phase correction similar to Chariklo's  $G = 0.15$  (McBride et al. 1999). We corrected the September and November data magnitudes taken at viewing phase angles of  $\alpha$  by shifting the magnitudes by a value of  $\delta m$ , where

$$\delta m = \Delta m(4^\circ) - \Delta m(\alpha), \quad (1)$$

$$\Delta m(\alpha) = 5 \log \left( \frac{\Delta}{\Delta_{12/18}} \frac{r}{r_{12/18}} \right) - 2.5 \log [(1 - G)\Phi_1(\alpha) + G\Phi_2(\alpha)], \quad (2)$$

and where  $\Phi_1$  and  $\Phi_2$  are approximated by

$$\Phi_1 = \exp \left\{ -3.33[\tan(0.5\alpha)]^{0.63} \right\}, \quad (3)$$

$$\Phi_2 = \exp \left\{ -1.87[\tan(0.5\alpha)]^{1.22} \right\} \quad (4)$$

(Bowell et al. 1989). PDM analysis of the resulting light curve showed a sharper minimum at 13.3 hr, consistent with the period of 13.25 hr reported by Gutiérrez et al. (2001) from data acquired at Calar Alto Observatory (CAO). We found an amplitude of  $0.095 \pm 0.015$  mag. To get an analytical value for the phase-curve  $G$  value and brightness at  $\alpha = 0^\circ$ , we removed the rotational light-curve offsets by fitting sine-curve functions with free variables of amplitude and magnitude offset to the UH 2.2 m September, November, and December data rephased to the 13.3 hr rotation period. As further constraint, we added in a data point derived from the minimum in the 2001 January 21 value from Gutiérrez et al. (2001). We did not use this in our period search, as our derived values for this point had uncertainties of 0.044 mag, almost half our light-curve amplitude, owing to possible filter bandpass discrepancies and those data's own reported statistical uncertainty, but we did use this value in our phase-curve fit iteration. After convolving the reported UH Kron-Cousins and CAO Bessel filter bandpasses<sup>3</sup>

<sup>2</sup> <http://ssd.jpl.nasa.gov/horizons.html>.

<sup>3</sup> <http://www.oan.es/1.52m/e/ccd.html>.

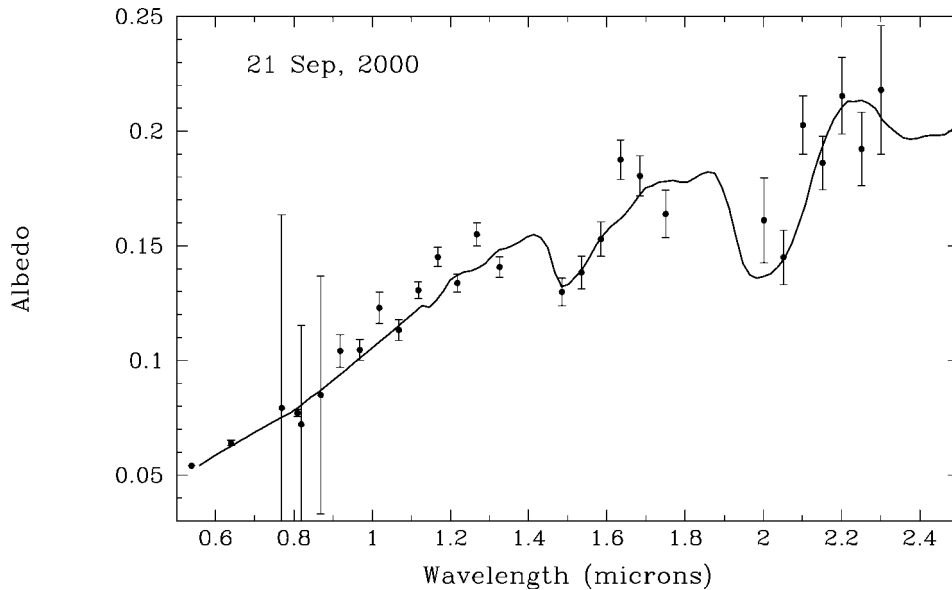


FIG. 7.—IRTF SpeX spectrum from 2000 September 21. The data are rebinned to 3 times the instrumental resolution and scaled to a 5% mean optical albedo at V-band wavelengths. The September 21 compositional model with the lowest  $\chi^2$  from Table 7 is shown here (*solid line*) and is composed of amorphous water ice, amorphous carbon, and Titan tholins.

with the solar spectrum, we found a  $0.0064 \mu\text{m}$  offset in effective  $R$  wavelength and calculated a  $0.04 (\pm 0.01)$  mag offset between our reported  $R$ -band magnitudes and those from Gutiérrez et al. (2001). We found that a similar correction was necessary for the McDonald Observatory data as well, as they use similar filter bandpasses. For the period search and phase-

curve analysis, it was easier to shift the McDonald Observatory and CAO data sets to the UH Kron-Cousins filter system.

Our first iteration yielded  $G = -0.14$ . Because of the large offset from the initial guess of  $G = 0.15$ , in order to untangle the effects of the viewing angle phase from the rotational phase, we decided it was necessary to use an iterative procedure as

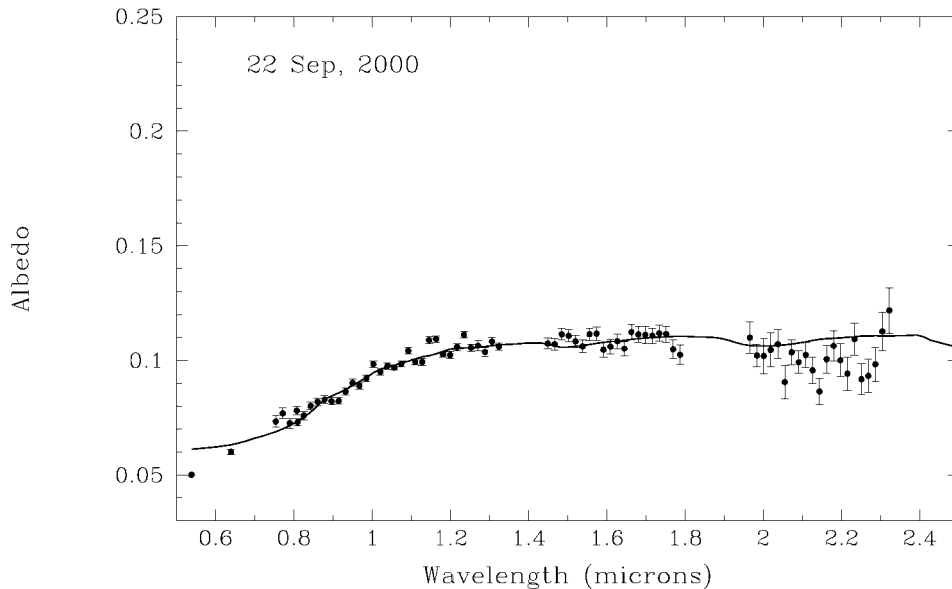


FIG. 8.—IRTF SpeX spectrum from 2000 September 21. The data are rebinned to the instrumental resolution and scaled to a 5% mean optical albedo at V-band wavelengths. The September 22 compositional model with the lowest  $\chi^2$  from Table 7 is shown here (*solid line*) and is comprised of amorphous water ice, amorphous carbon, Triton tholins, methanol ice, and olivine.

follows. (1) Assume a value for  $G$  and correct all data sets with the phase law described by this value. (2) Find the best-fitting rotational period and amplitude. (3) Find the mean brightness (over a rotation period) in each data set and shift the magnitudes to account for this. (4) Refit for  $G$ . Readjusting our data using the new  $G$  values, we conducted the period searches using a Fourier periodogram technique, in place of the earlier PDM technique. We also employed an algorithm called WINDOW CLEAN developed by Belton (1990), which eliminated false peaks introduced by the regular sampling of the data. On our fourth iteration, we found a period of  $13.413 \pm 0.04$  hr, which was well within the uncertainty of the previous value of 13.408 hr. We adopt the value of  $13.41 \pm 0.04$  for the light-curve period. The Fourier spectra, raw and cleaned using Belton's (1990) technique, are shown in Figure 1. Our December data are shown in Figure 2, with a sine curve of period 13.41 hr superposed. Our total light-curve data, phased to the 13.41 hr period, are shown in Figure 3 and show an amplitude of  $0.102 \pm 0.005$ , based on a weighted average of the points about the peak and trough. An alternative rotation period of 26.82 hr may be possible if the brightness variation is caused by shape rather than surface albedo features (Fig. 4). We found final phase-curve parameters of  $G = -0.13 \pm 0.02$  and  $m_r(\alpha = 0)$  of  $18.45 \pm 0.02$ , using the standard deviation of our values in the successive iterations to determine our uncertainties. Using the UH 2.2 m data alone, our fit for  $G$  becomes  $-0.122 (\pm 0.06)$  and  $18.46 (\pm 0.03)$  for  $m_r(\alpha = 0)$ , well within the errors of the final value we report. Figure 5 shows the phase curve and fitted magnitude points of our three data sets, along with the magnitude value from Gutiérrez et al. (2001). Because of the relatively high uncertainties in the 2000 August data and the large temporal gap between our 2000 and the 2001 October data, we did not use these data sets to constrain our fits for either the rotational phase or the viewing-angle Lumme-Bowell model. However, we do include these data in Figure 5 for comparison. For the plot, we corrected the 2000 August data point for the approximate rotational phase ( $\phi_{\text{rot}} \approx 0.66$ ) based on the period derived from the previous data sets.

We derived  $BVRI$  colors from our data by averaging the  $R$ -band values bracketing our  $B$ -,  $V$ -, and  $I$ -filter observations and using  $R$  as our reference filter for our magnitude differences. In order to compare data sets more easily with prior literature values, we converted our UH filter set colors to Bessel filter set values (Bessel 1990). Table 5 shows the effective wavelengths of the filter sets, as derived by convolving the filter bandpass with a solar spectrum. Also shown are the final offset values we used to convert the UH 2.2 m colors to values similar to those obtained with the CAO and McDonald Observatory filter sets. For the special case of the 2000 August data, obtained with the 8K mosaic camera, we included the 0.022 offset in the reported  $V-R$  colors. However, we fold in an equivalent value into the reported uncertainty because the filter set is not as well calibrated as that provided with the Tek

2K camera. Table 6 shows the final colors and color gradients. The color gradient for each Centaur is expressed in terms of the slope parameter, as defined in Hainaut & Delsanti (2002), which is the percent of reddening, with respect to solar colors, per 0.1  $\mu\text{m}$ . Our values were derived using the equation

$$[\% \text{ gradient}] = (10^{0.4(\Delta m_{\text{obj}} - \Delta m_{\odot})} - 1) / \Delta \lambda, \quad (5)$$

where  $\Delta m_{\text{obj}}$  is the Centaur's color for a particular filter pair,  $\Delta m_{\odot}$  is the corresponding solar color for that filter pair, and  $\Delta \lambda$  is the difference in the filter pair's effective wavelengths in units of 0.1  $\mu\text{m}$ . The listed gradients are based upon the central wavelengths for the Bessel filter color values. We find no correlation with rotational phase or viewing phase angle. We also include those reported by Gutiérrez et al. (2001), shown in Figure 6.

### 3.2. Spectroscopy

We used the Spextool package written by M. Cushing<sup>4</sup> to reduce the data, following the suggested procedure for faint sources. This included flattening the data with quartz-lamp flats, removing known bad pixels and mosaic defects, and wavelength calibrating the data with argon-lamp exposures and sky lines. Prior to combining the exposures, we removed cosmic rays by hand. We divided the spectra by our G5 V standard. Our slit size, 0".8, corresponded to an approximately 5 pixel width in the dispersion direction. These data, then, were inherently oversampled, and as a result we averaged 5 pixels into a single bin value for the data taken on September 22. For the case of the September 21 data, we rebinned this spectrum to nearly one-third the resolution to achieve a higher signal value per bin. Hence, for the September 21 data, 14 pixels were averaged into a single bin value to obtain a signal-to-noise ratio (S/N) more closely comparable to that from September 22.

We present here the first attempts at modeling the data. In order to provide insight into the nature of the surface material(s) on 1999 UG<sub>5</sub>, we have produced model spectral albedos for different candidate materials and their associated grain size(s) to compare with the new data. The model used is that originally developed by Hapke (1993) to describe the measured albedo. The details describing the formulation used in our effort are provided by Roush et al. (1990), Roush (1994), and Cruikshank et al. (1998). The limited phase-angle coverage of NIR wavelengths precludes us from independently determining some of the parameters of the models. Here we rely upon values of these parameters derived from *Voyager* observations for the outer solar system moon of Miranda by Helfenstein, Veverka, & Thomas (1988), which would be appropriate for a porous or fluffy surface; specifically, the parameters, as defined by Roush (1994), have the values  $b = 0.93$ ,  $h = 0.018$ , and  $S_0 = 0.77 \times$  (Fresnel reflectance). This approach also requires

<sup>4</sup> <http://irtfweb.ifa.hawaii.edu/Facility/spex/Spextool.txt>.

that the real and imaginary indices of refraction of candidate materials be specified. The availability of appropriate optical constants is limited, constraining our range of model computations.

The first night's data were of notably poorer quality than the second night's, so we fitted a simple three-component intimate mixture model to the data using the scattering code. The presence of absorption features at 1.5 and 2.0  $\mu\text{m}$  corresponded to features found in water-ice spectra. The lack of a secondary absorption dip near 1.65  $\mu\text{m}$  seemed to indicate that the amorphous form of water ice, rather than the crystalline form, would provide a better fit. Attempts to include crystalline water ice in the fits were unsuccessful and would not converge. We included tholin material in the hope of fitting the redward gradients in both spectra. Triton tholin, which has a redward gradient that extends farther into longer wavelengths, provided a better fit than Titan tholin, which has a reflectance that plateaus near 1.3  $\mu\text{m}$ . Based on albedo measurements of other Centaurs (e.g., Fernández, Jewitt, & Sheppard 2002), all our spectral data were rescaled to a 5% visual albedo. However, the fits were not rescaled, so a neutral absorber with a flat reflectance across the observed wavelengths was incorporated into the fits in the form of amorphous carbon. For the case of the September 21 data, more species other than amorphous carbon, amorphous water ice, and Triton tholin in the intimate mixtures produced poorer fits (e.g., Table 7). This simpler three-species combination, which resulted in the best-fit model for the September 21 data, yielded a poorer model fit for the September 22 data, with reduced  $\chi^2$  values equal to 5.12. Owing to the similarity in color to Pholus, for the September 22 data, we tried a five-component intimate mixture similar to that used to fit the Pholus spectra reported by Cruikshank et al. (1998). Here Titan tholin provided a better fit. Variations from this model again produced poorer fits with reduced  $\chi^2$  values ranging from 4.4 to 10. The fitting results are summarized in Table 7. The data and model fits with the lowest  $\chi^2$  values, with amorphous water ice, amorphous carbon, and Triton tholin for September 21, and with amorphous water ice, amorphous carbon, methanol, Titan tholin, and olivine for September 22, are shown in Figures 7 and 8. The fitting for the model species and abundances are based on weighted fits of the data shown. Hence, in both cases, the model fits are poorer at longer wavelengths, where there is lower S/N due to higher sky background.

#### 4. DISCUSSION

Our light-curve analysis shows that the rotation of 1999 UG<sub>5</sub> causes a  $13.41 \pm 0.04$  hr period in the observed brightness variation and exhibits a light-curve amplitude of  $0.102 \pm 0.005$  mag. These results are more precise than those of Gutiérrez et al. (2001) but are consistent to within their quoted uncertainties. This would also be consistent with either a 26.82 hr rotation of an ellipsoid with a 1.25 axis ratio or a 13.41 hr rotation of a body with a bright surface feature. The latter case may be a

better interpretation given the observed variation in the NIR surface spectrum, although the variations do not perfectly phase with the brightness peak (see Fig. 3). The addition of many nights of data, spanning 12 weeks, also seems to indicate that there is no complex component to the rotation. In other words, it is in simple rotation, at least on timescales of several months. We at first suspected that the peak data point in the 2000 December light curve was anomalous. However, when we added the phased November 1–2 data taken at McDonald Observatory, we found a correspondingly bright peak data point. In any case, we are confident that the light-curve peak has an irregular shape, which may be attributable to either an irregular asymmetric geometric shape or surface albedo features. Furthermore, the irregular shape of the peak persists with the 26.82 hr rotation period (Fig. 4).

We find a redder surface on average than previously reported but still within typical values of the Centaurs. We also find a less steep color gradient at  $V-R$  wavelengths ( $11.1\% \pm 2.0\%$ ), based on the weighted average of all our  $V-R$  colors ( $0.68 \pm 0.02$ ), than at  $R-I$  wavelengths ( $13.8\% \pm 1.2\%$ ,  $R-I = 0.58 \pm 0.02$ ), which is typical for transneptunian objects (e.g., Boehnhardt et al. 2002). This trend in the color gradients is consistent with the Gutiérrez et al. (2001) results. We find no trend in colors with rotation. There are instances across our total data set where the measured color values vary by as much as one-sixth the mean value, but most of the values we report have overlapping error bars. There is a tendency for the observations on nights with thin cirrus present to yield the reddest values of the  $V-R$  color data. However, the data from November 2 were taken on a photometric night. Subsequent examination of optical photometry yielded no systematic sources of error that would not be compensated for by our reduction methods, at least to the level of the reported accuracy of the measurements. Hence, we attribute these deviations to primarily statistical noise.

McBride et al. (1999) reported a phase curve for the Centaur Chariklo with a Lumme-Bowell  $G$ -slope parameter of 0.15. This parameter corresponds to the steepness of the slope of the phase brightening, particularly at angles greater than a few degrees, and is often interpreted as an indication of porosity. A lower  $G$  value indicates a steeper slope and a possibly more porous surface. Our derived value of  $G = -0.13$  is an unusually low value for a small body, but not unprecedented. Comet P/Encke's value was reported by Fernández et al. (2000) as  $-0.25$ , and negative values have been found for some Kuiper belt objects (Sheppard & Jewitt 2002). As with cometary bodies, larger porosity may be the consequence of volatile liberation. Our 2000 December 18 reference frame value of  $m_r(\alpha = 0) = 18.45$  for our data fits yields an  $H_r(0, 1) = 10.32$  and a diameter of 58 km, assuming an albedo of 0.05, as reported for Pholus and Chariklo, or 37 km, assuming a 0.12 albedo value similar to Asbolus's (Fernández et al. 2002).

The two spectra we presented show surprisingly different features. The September 22 spectrum is near a rotational light-

curve phase of 0.37, and the September 21 is near a rotational phase of 0.64, slightly closer to the peak in brightness, given a single-peak rotation. As much as 56% of the surface would be different in this case. A double-peaked light curve is harder to explain with the observed spectral differences, as the phases are closer together at 0.37 and 0.51, and only as much as 28% of the surface would be different between the two spectra. However, a 26.82 hr rotation period would place the September 21 spectrum squarely at the peak in brightness. The September 21 spectrum also shows the strongest possible water-ice signatures, at 2.0 and 1.55  $\mu\text{m}$ , which may correlate nicely with a peak in brightness if it is all caused by exposed water ice. Because of the poor S/N and the brief integration time, we are reluctant to call this a detection. Furthermore, deviations of our model fits from the data at 1.63 and 2.1  $\mu\text{m}$  may suggest that other species not accounted for are in abundance. It also seems likely that the slope is indeed redder at NIR wavelengths in this region of the surface. The turnover in the September 22 spectrum (and likely absorption feature) extending beyond 2.0  $\mu\text{m}$  does not correspond to a water-ice feature, but rather some other material, or combination of materials, possibly organic, is likely the cause. In any case, that the possible water-ice band is on a redder and brighter region of the surface is somewhat surprising. Reddening by radiation aging (Strazzulla & Johnson 1991) and grayer colors corresponding to fresh ice exposed by impacts or redeposited after cometary activity (Stern 1995; Hainaut et al. 2000) may yield a different expectation. The extremely red colors of the active Centaur object 2001 T<sub>4</sub> (Bauer et al. 2001) would also seem to support a different interpretation. 1999 UG<sub>5</sub> is at an appropriate distance for com-

etary activity. It has similar orbital parameters as Chiron and evidence of water, possibly in amorphous ice form. If the appropriate volatiles are trapped in the ice, it may very well undergo cometary activity on a periodic basis (e.g., Prialnik, Brosch, & Ianovici 1995), although we do not witness it at the present.

1999 UG<sub>5</sub>, at first an apparently ordinary Centaur, poses many interesting possible exceptions to several of the currently held interpretations of observed Centaur phenomena. It is worthy of further study. Higher S/N NIR spectra, well correlated with the optical behavior of the Centaur, would especially be desirable. Indeed, many of the Centaurs, even those already observed in the NIR, are in need of such a correlated optical and NIR study, so that we may determine whether the Centaur class as a whole is populated more with diverse exceptions than with examples of inferred rules.

The authors of this paper would like to acknowledge the staff at the UH 2.2 m and NASA IRTF telescopes, especially John Dvorak, Dave Griep, and Bill Golish, whose efforts during the observations were critical to their success. Scott Sheppard and Peter Capak very ably assisted in obtaining the UH 2.2 m data on the nights of November 8 and September 22, respectively. We would also like to thank Marc Buie of Lowell observatory, who provided us with the original PDM code, Michael Cushing and William Vacca for their Spextool reduction package code and SpeX data reduction assistance, and John Rayner for the overall instrument development and support. J. M. B. acknowledges support for this work from the planetary astronomy program NAG 5-4495.

## REFERENCES

- Barrucci, M. A., Lazzarin, M., & Tozzi, G. P. 1999, *AJ*, 117, 1929  
 Barrucci, M. A., et al. 2002, *A&A*, 392, 335  
 Bauer, J. M., Meech, K. J., Owen, T. C., Roush, T. L., & Dahm, S. E. 2001, *BAAS*, 33, 1212  
 Belton, M. J. S. 1990, *Icarus*, 86, 30  
 Bessel, M. S. 1990, *PASP*, 102, 1181  
 Bevington, P. R. 1969, *Data Reduction and Error Analysis for the Physical Sciences* (New York: McGraw-Hill), 202  
 Boehnhardt, H., et al. 2002, *A&A*, 395, 297  
 Bowell, E., Hapke, B., Domingue, D., Lumme, K., Peltoniemi, J., & Harris, A. 1989, in *Asteroids II*, ed. R. P. Binzel, T. Gehrels, & M. S. Matthews (Tucson: Univ. Arizona Press), 525  
 Brown, M. E., & Koresko, C. D. 1998, *ApJ*, 505, L65  
 Brown, W. R., & Luu, J. X. 1997, *Icarus*, 126, 218  
 Buie, M. W., & Bus, S. J. 1992, *BAAS*, 24, 0601  
 Bus, S. J., Bowell, E., & French, L. M. 1988, *IAU Circ.*, 4684, 2  
 Cruikshank, D. P., et al. 1998, *Icarus*, 135, 389  
 Farnham, T. L. 2001, *BAAS*, 33, 3104  
 Farnham, T. L., & Davies, J. K. 2002, *Icarus*, submitted  
 Fernández, Y. R., Jewitt, D. C., & Sheppard, S. S. 2002, *AJ*, 123, 1050  
 Fernández, Y. R., et al. 2000, *Icarus*, 147, 145  
 Foster, M. J., Green, S. F., McBride, N., & Davies, J. K. 1999, *Icarus*, 141, 408  
 Gaidos, E. J. 1998, *PASP*, 110, 1259  
 Gutiérrez, P. J., Ortiz, J. L., Alexandrino, E., Roos-Serote, M., & Doressoundiram, A. 2001, *A&A*, 371, L1  
 Hainaut, O. R., & Delsanti, A. C. 2002, *A&A*, 389, 641  
 Hainaut, O. R., et al. 2000, *A&A*, 356, 1076  
 Hapke, B. 1993, *Reflectance and Emittance Spectroscopy* (New York: Cambridge Univ. Press), 455  
 Helfenstein, P. J., Veverka, J., & Thomas, P. C. 1988, *Icarus*, 74, 231  
 Holman, M. J., & Wisdom, J. 1993, *AJ*, 105, 1987  
 Jedicke, R., & Herron, J. D. 1997, *Icarus*, 127, 494  
 Kern, S. D., McCarthy, D. W., Buie, M. W., Brown, R. H., Campins, H., & Rieke, M. 2000, *ApJ*, 542, L155  
 Landolt, A. U. 1992, *AJ*, 104, 340  
 McBride, N., Davies, J. K., Green, S. F., & Foster, M. J. 1999, *MNRAS*, 306, 799  
 Ortiz, J. L., Baumont, S., Gutiérrez, P. J., & Roos-Serote, M. 2002, *A&A*, 388, 661  
 Peixinho, N., Lacerda, P., Ortiz, J. L., Doressoundiram, A., Roos-Serote, M., & Gutiérrez, P. J. 2001, *A&A*, 371, 753  
 Prialnik, D., Brosch, N., & Ianovici, D. 1995, *MNRAS*, 276, 1148  
 Romon-Martin, J., Barucci, M. A., de Bergh, C., & Peixinho, N. 2001, *BAAS*, 33, 0805  
 Roush, T. L. 1994, *Icarus*, 108, 243  
 Roush, T. L., Pollack, J. B., Witteborn, F. C., Bregman, J. D., & Simpson, J. P. 1990, *Icarus*, 86, 355

- Sheppard, S. S., & Jewitt, D. C. 2002, AJ, 124, 1757  
Sheppard, S. S., Jewitt, D. C., Trujillo, C. A., Brown, M. J. I., & Ashley, M. C. B. 2000, AJ, 120, 2687  
Stellingwerf, R. F. 1978, ApJ, 224, 953
- Stern, S. A. 1995, AJ, 110, 856  
Strazzulla, G., & Johnson, R. E. 1991, in Comets in the Post Halley Era, ed. R. L. Newburn (Dordrecht: Kluwer), 243  
Tegler, S. C., & Rominishin, W. 2000, Nature, 407, 979